



## Short communication

Enhanced Pt utilization in electrocatalysts by covering of colloidal silica nanoparticles<sup>☆</sup>Jianhuang Zeng<sup>a,\*</sup>, Jianjun Chen<sup>a</sup>, Jim Yang Lee<sup>b</sup><sup>a</sup> C711, Center for Advanced Materials & Biotechnology, Research Institute of Tsinghua University in Shenzhen, Shenzhen High-Tech Industrial Park, Shenzhen, Guangdong 518057, China<sup>b</sup> Department of Chemical and Biomolecular Engineering, National University of Singapore, 10 Kent Ridge Crescent, Singapore 119260, Singapore

## ARTICLE INFO

## Article history:

Received 4 January 2008

Received in revised form 26 February 2008

Accepted 2 April 2008

Available online 8 April 2008

## Keywords:

Pt utilization

Electrocatalysts

Silica

Methanol electro-oxidation

## ABSTRACT

This work aims at enhancing Pt utilization in electrocatalysts by covering of preformed silica nanoparticles. Pt/C electrocatalysts were prepared by reductive deposition of Pt by citrate at moderate temperatures on silica nanoparticles with varying atomic silica to Pt ratios (1.7:1 and 3.3:1) to study the effects of silica to Pt ratio. Considerable voidages were created by inter-situated 10–20 nm silica nanoparticles between support carbon particulates to facilitate mass transfer of reactants and products. This particular method of catalyst preparation increases the Pt metal utilization, and generates a large amount of accessible voidage in the interpenetrating particle network of carbon and silica to support the facile transport of reactants and products. Electrochemical hydrogen adsorption/desorption has shown an increase in electrochemically active surface area by this approach. Methanol electro-oxidation was used as a test reaction to evaluate the catalytic activity. It was found that the Pt catalyst modified with silica at silica:Pt = 1.7:1 atomic ratio was more active than a catalyst prepared when silica to Pt ratio increased to 3.3:1.

© 2008 Elsevier B.V. All rights reserved.

## 1. Introduction

One of the key issues that hinder the commercialization of proton-exchange membrane fuel cells (PEMFC) is the high cost of precious metal electrocatalysts [1,2]. Platinum is widely used as catalysts for hydrogenation, auto exhaust, fuel cells, etc. In view of the scarce resources and limited reserve (around 65,000 tonnes) of platinum, researchers nowadays turned their attention to the Pt utilization enhancement in heterogeneous catalysis. A high-surface-to-mass ratio provided by small metal nanoparticles is certainly desirable on grounds of improved metal utilization in fuel cell community. However, not all geometric specific-surface area contributes to the heterogeneous catalysis, only a minority of electrocatalysts is electrochemically active while an overriding majority of the noble metal nanoparticles are not accessible to reactions. The lost activity thus negates the merits of small nanoparticles and the effort in producing them. Wilson et al. observed that particle ripening was evident when supported Pt catalyst ran 4000 h in life tests of PEMFC [3]. They reported that the initial Pt specific-surface area

dropped to 40–50% in the cathode and 60–70% in the anode through X-ray diffraction analyses.

Zhao et al. employed gold nanoparticles of varying sizes as underlying metal to deposit Pt nanoparticles and found the mass catalytic activity of Pt@Au/C improved significantly [4,5]. Xi et al. reported a simple approach to enhance Pt utilization and CO-tolerance by mixing Pt/C catalysts with transition metal oxide (TMO) such as CeO<sub>2</sub>. They argued that the diluting effect of TMO in the catalysts structure led to ready access of reactant to the catalysts consequently enhanced Pt utilization [6]. We have also reported a method to enhance Pt utilization by firstly depositing Pt nanoparticles on colloidal silica (Pt-silica), followed by the adsorption of the latter onto a carbon support [7]. In our approach we employed silica nanoparticles of proper sizes (~20 nm) to situate in the interstitial gap enclosed by surrounding supported-carbon particulates. Introduction of silica nanoparticles can resist carbon agglomeration and thereby most of the Pt surface area can be participated in the oxidation reaction. Herein we present the effects of silica to Pt ratio in the preparation on the improvement of mass activity towards methanol oxidation in acidic media at room temperature.

## 2. Experimental

Hydrogen hexachloroplatinate(IV) hydrate from Aldrich, sodium citrate, sodium borohydride, sulfuric acid (95–97%)

<sup>☆</sup> The work was supported by China Postdoctoral Science Foundation (funding no. 20070420805).

\* Corresponding author. Tel.: +86 755 26551374; fax: +86 755 26551338.  
E-mail address: [jhzeng@gmail.com](mailto:jhzeng@gmail.com) (J. Zeng).

and methanol from Merck, and Snowtex-C colloidal silica from Nissan Chemical Industries were used as received without further purification. De-ionized water was used throughout the investigation.

The preparation of Pt–silica/C was similar to that of the previously reported Pt–silica/C [7]. In brief: a mixture of 1 ml 0.05 M  $\text{H}_2\text{PtCl}_6$ , 5 ml  $1 \text{ mg ml}^{-1}$  colloidal silica and 2.5 ml 0.05 M sodium citrate were introduced to a 250 ml flat-bottom flask fitted with a condenser. De-ionized water was used to top up the content to 200 ml. The mixture was heated at  $70^\circ\text{C}$  in an oil-bath and placed under reflux with stirring for 12 h. Seventy milligrams of the processed carbon was added to the reaction mixture after cooling (named Pt–silica hereafter) while stirring continued overnight for the light yellow sol. The suspension was then filtered to recover the solid, which was copiously washed with water before drying in vacuum at  $40^\circ\text{C}$  overnight. Different to our previously reported preparation method, the catalysts were heat treated in a tubular furnace for 1 h at  $300^\circ\text{C}$  to remove the possible citrate residue on Pt nanoparticles. In doing this, high-purity Ar ( $0.5 \text{ l min}^{-1}$ ) was flushed 1 h before heating and kept until cooling to room temperature. The catalyst is named Pt–silica-1/C (the silica to Pt atomic ratio is 1.7:1). Pt–silica-2/C is similarly prepared but with  $10 \text{ ml } 1 \text{ mg ml}^{-1}$  colloidal silica in preparation (the silica to Pt atomic ratio is 3.3:1).

Information on particle size, shape and size distribution was obtained with a JEOL JEM2010 transmission electron microscope (TEM) operating at 200 kV. X-ray powder diffraction (XRD) patterns of the catalysts were recorded by a Rigaku D/Max-3B diffractometer (SHIMADZU), using Cu  $K\alpha$  radiation ( $\lambda = 1.5406 \text{ \AA}$ ). The  $2\theta$  angles were scanned from  $20^\circ$  to  $85^\circ$  at  $4^\circ \text{ min}^{-1}$ . The diffraction data was curve fitted by a least-square program provided by the equipment manufacturer. Elemental compositions were determined by an EDX analyzer attached to a JEOL MP5600LV scanning electron microscope (SEM) operating at 15 kV. Surface compositions were obtained by X-ray photoelectron spectra (XPS). The XPS were obtained from an ESCALAB MKII spectrometer (VG Scientific) using Al  $K\alpha$  radiation (1486.71 eV). Spectral correction was based on the graphite C 1s level at 284.5 eV [8]. The vendor-supplied XPSPEAK version 4.1 was used to deconvolute all XPS data, using fixed half widths and fixed spin orbit splitting in first trials.

An Autolab PGSTAT12 potentiostat/galvanostat, and a standard three-electrode electrochemical cell were used to evaluate the catalyst activity by cyclic voltammetry. The working electrode was a 5 mm diameter glassy carbon disk electrode cast with a catalyst ink in Nafion solution. Pt gauze and a saturated Ag/AgCl electrode were used as the counter electrode and the reference electrode to complete the circuit. All potentials are therefore referenced to the Ag/AgCl electrode. Methanol was used as a probe molecule to evaluate the catalyst activity. The electrolyte used was 1 M  $\text{CH}_3\text{OH}$  in 0.5 M  $\text{H}_2\text{SO}_4$ . Voltammograms at  $20 \text{ mV s}^{-1}$  were recorded after a stable response was established.

### 3. Results and discussions

Fig. 1 shows the TEM image of Pt–silica-1 and Pt–silica-2 sol. The larger (around 20 nm) particles are colloidal silica and the smaller (1.5–2.3 nm) ones are Pt nanoparticles. It can be seen that some Pt nanoparticles were off the silica substrate in Fig. 1a and Pt nanoparticles were all deposited on the silica support as shown in Fig. 1b. There were no observable particle size difference for the sol and the overall Pt particle size distribution was broad with a mean diameter of 1.8 nm. The condition favoring Pt particle deposition on silica was a slow and controlled reaction rate. Sodium citrate was a weak reducing agent compared with most of the conventionally used

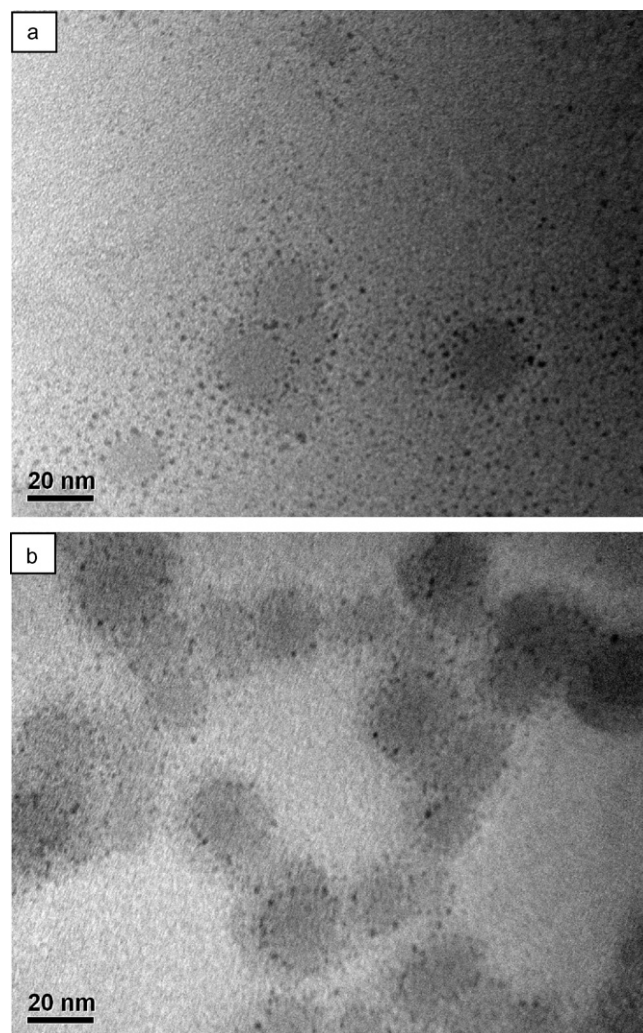


Fig. 1. TEM images of colloidal (a) Pt–silica-1 and (b) Pt–silica-2.

reducing agent such as  $\text{NaBH}_4$  and the deposition of Pt had to be initiated at elevated temperatures ( $70^\circ\text{C}$  in this experiment). When silica to Pt atomic ratio increased from 1.7:1 to 3.3:1, more heterogeneous nucleation centers favored the deposition of Pt on silica substrate therefore all Pt nanoparticles were deposited on silica as in Fig. 1b.

Fig. 2 shows the XRD patterns for both catalysts. The characteristic (1 1 1) peak at  $2\theta$  value of  $39.8^\circ$  can be observed for the catalysts and the (2 0 0), (2 2 0) and (3 1 1) diffractions are weak and not obvious probably due to the small particle size effect. The characteristic face-centered cubic Pt diffraction peaks became sharper when the post-heating temperature increased to  $600^\circ\text{C}$  due to the increased Pt particle sizes. The post-treatment temperature was kept at  $300^\circ\text{C}$  in this work to prevent particle sintering.

Table 1  
Quantification report of the catalysts by XPS analyses

Peak	Binding energy (eV)	Atomic concentration (%)	
		Pt–silica-1/C	Pt–silica-2/C
O 1s	532.45	4.21	7.77
C 1s	284.50	95.10	90.01
Si 2p	102.40	0.45	1.74
Pt 4f	72.95	0.24	0.48

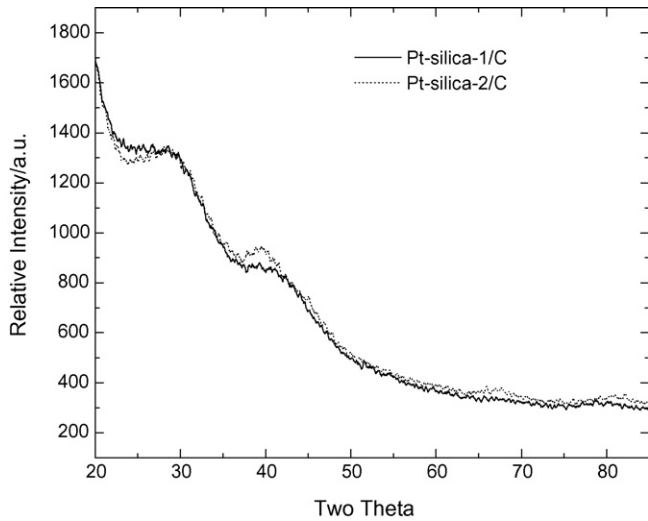


Fig. 2. XRD patterns of Pt-silica-1/C and Pt-silica-2/C catalysts.

The Pt 4f XPS spectra of the catalysts are shown in Fig. 3. The quantification report is given in Table 1. In Table 1, the atomic ratio of silica to Pt for Pt-silica-1/C and Pt-silica-2/C is 1.9:1 (the nominal atomic ratio is 1.7:1 in preparation) and 3.6:1 (the nominal atomic

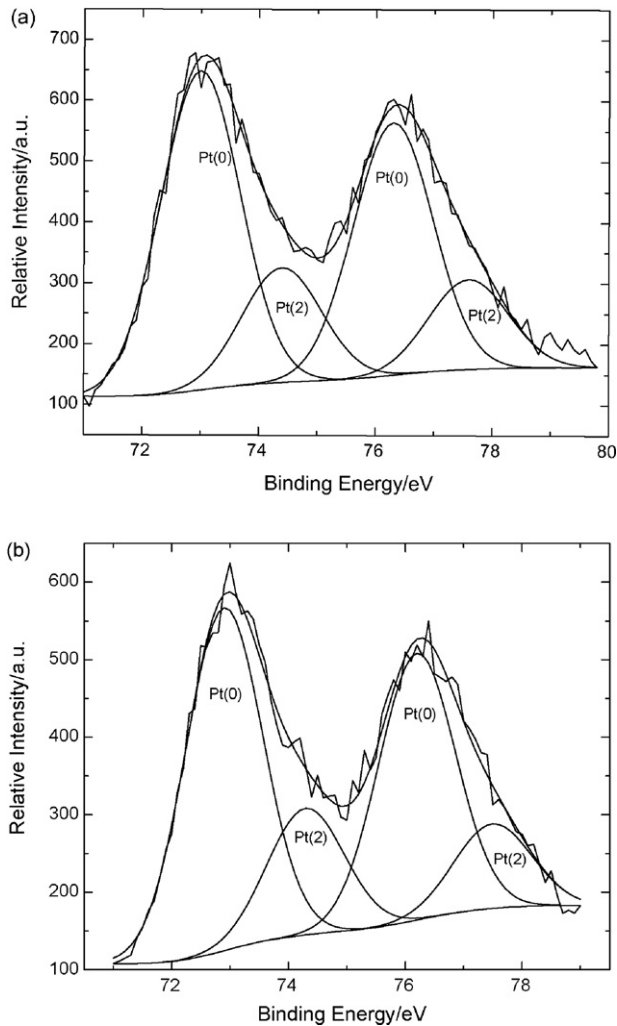


Fig. 3. XPS spectra in the Pt 4f region of the catalyst (a) Pt-silica-1/C and (b) Pt-silica-2/C.

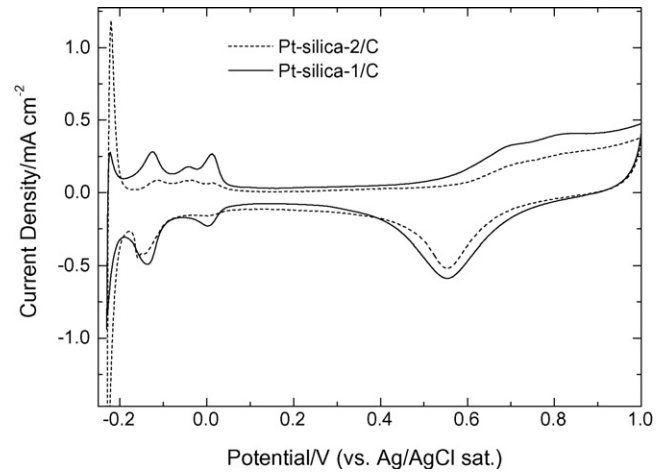


Fig. 4. Room temperature cyclic voltammograms of the catalysts measured at  $20 \text{ mV s}^{-1}$  in  $0.5 \text{ M H}_2\text{SO}_4$ .

ratio is 3.3:1 in preparation), respectively. The higher atomic ratio of silica to Pt in the catalysts relative to the nominal value in preparation is due to sampling depth (2–5 nm from surface) of the X-ray in XPS characterization [9]: the Pt nanoparticles are deposited on the silica substrate leading to higher sampling ratio relative to the silica substrate. The percentages of Pt(0) in both catalysts calculated from the integrated area intensities are around 74%. For the Pt-silica-1/C catalyst in Fig. 3a, the more intense doublet at 72.99 and 76.29 eV is a signature of metallic Pt (Pt(0)). The less intense doublet at 74.39 and 77.59 eV, on the other hand, is often attributed to oxidized Pt in the divalent states such as PtO and Pt(OH)<sub>2</sub> [10–12]. The Pt 4f XPS spectra of Pt-silica-2/C (Fig. 3b) were similarly deconvoluted. The shift in the Pt(0) peak to higher BE relative to the Pt standard could arise from metal-support (in this case: Pt-silica) interaction and/or small cluster-size effects [13].

Catalytic activity can be expressed in terms of specific mass activity (current per unit mass of catalyst), or specific activity, which uses the electrochemically active surface area (ECSA) to normalize the current [14]. The former reflects the effectiveness of catalyst preparation with respect to metal utilization, whereas the latter is more indicative of the intrinsic activity of the Pt sites. The ECSA of Pt catalysts can be estimated from the charge associated with hydrogen adsorption on Pt in Fig. 4 [14–17]. An electrolyte of  $0.5 \text{ M H}_2\text{SO}_4$  was used for the measurement. High-purity Ar was used before and during the measurement to deaerate the electrolyte. The baseline for the measured current was extended from the double-layer region of the cyclic voltammogram. The electrochemical surface area in  $\text{m}^2 \text{ g}^{-1}$  was calculated assuming a correspondence value of  $0.21 \text{ mC cm}^{-2} \text{ Pt}$  [18]. It can be found that the ECSA for Pt-silica-1/C is higher than that of the Pt-silica-2/C indicating better accessibility of reactants to the Pt catalysts.

Methanol electro-oxidation was used as a test reaction to evaluate the catalyst activities and the resulting cyclic voltammograms are shown in Fig. 5. Fig. 5 shows the cyclic voltammograms of room temperature electro-oxidation of methanol in  $1 \text{ M CH}_3\text{OH} + 0.5 \text{ M H}_2\text{SO}_4$  measured at a scan rate of  $20 \text{ mV s}^{-1}$ . The catalysts may be ranked by the peak current density at  $\sim 0.65 \text{ V}$  in the forward scan. The specific mass activity of Pt-silica-1/C and Pt-silica-2/C, as measured by the peak current density in the forward scan at  $0.65 \text{ V}$ , was 17 and  $15 \text{ mA cm}^{-2}$ , respectively. It may be noteworthy that the catalytic activity of Pt-silica-1/C is higher than that of Pt-silica/C reported previously [7] indicating that the post heat treatment of the catalyst effectively removed the possible citrate residue in the surface.



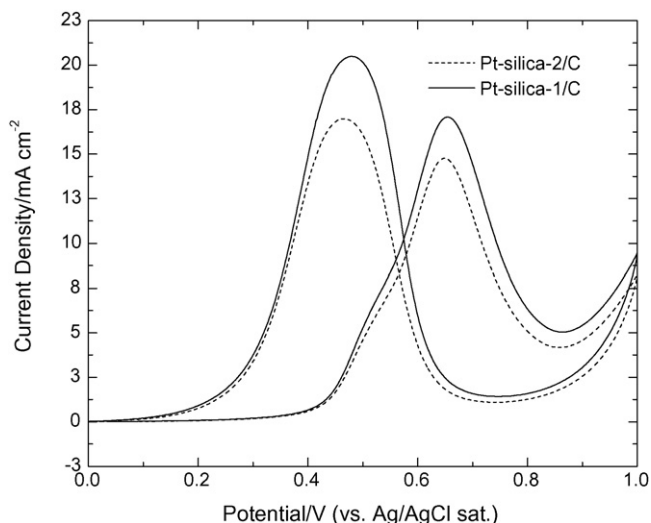


**Fig. 5.** Room temperature cyclic voltammograms of catalysts in 1 M  $\text{CH}_3\text{OH} + 0.5 \text{ M H}_2\text{SO}_4$  at a scan rate of  $20 \text{ mV s}^{-1}$ .

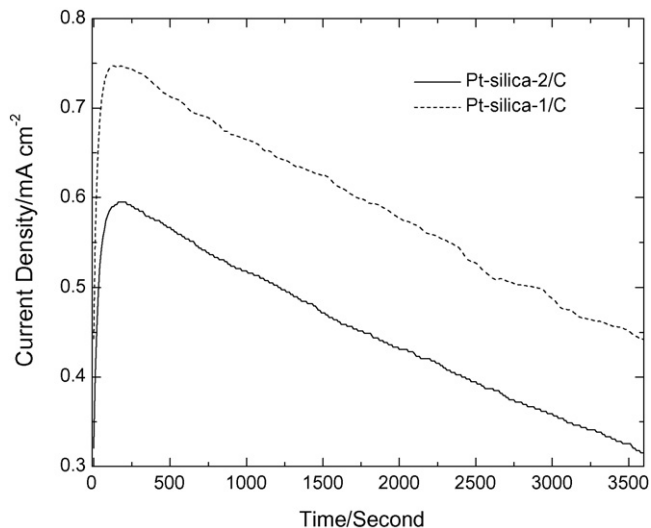


**Fig. 6.** Chronoamperograms of the catalysts at 0.35 V in 1 M  $\text{CH}_3\text{OH} + 0.5 \text{ M H}_2\text{SO}_4$  at room temperature.

Fig. 6 compares the chronoamperograms (CA) of the catalysts at 0.35 V. With the potential fixed at 0.35 V, methanol was continuously oxidized on the catalyst surface and tenacious reaction intermediates such as  $\text{CO}_{\text{ads}}$  would begin to accumulate if the kinetics of the removal reaction could not keep pace with that of methanol oxidation [19]. Fig. 6 shows that the oxidation current density decay rate of both catalysts is similar, around 55%. The decay rate is comparable to that of self-made PtCoW/C catalyst previously reported under identical conditions [20]. The slower decay rate of the silica-supported catalysts is due to the facile mass transport of the reactants and Pt–silica interactions.

The colloidal silica used for the preparation was about 20 nm in diameter. Particles in this size range were able to fit between

carbon particles ( $\sim 50 \text{ nm}$  in diameter) to form continuous channels extending throughout the interpenetrated network of silica and carbon particles. In this work, the amount of silica support has to be carefully controlled for the probable interruption of electrical path for electron transport in the electro-oxidation reaction though silica was not interfaced directly to carbon. In our previous report we predicted that Pt–silica-1/C (with the number of carbon and silica particles was calculated to be 1:1 and atomic ratio of silica to Pt is 1.7:1) could create an ideal case where the carbon particles would be in contact with each other with their interstitial void filled by Pt–silica particles. Although all Pt nanoparticles were deposited on the silica support when the initial silica amount increased twice (from silica to Pt atomic ratio = 1.7:1 increased to 3.3:1) as shown in Fig. 1b, the resulted Pt–silica-2/C catalyst is less accessible to reactants. The higher ECSA for Pt–silica-1/C and consequently better catalytic activity towards methanol oxidation relative to Pt–silica-2/C confirmed our prediction.

#### 4. Conclusions

Pt–silica nanoparticles were prepared by covering of preformed colloidal silica nanoparticles and used for methanol electro-oxidation catalysts aiming for enhanced Pt utilization. Silica to Pt atomic ratio was varied from 1.7:1 to 3.3:1 to study the effects on catalytic activity. The Pt deposition on or off silica substrate can be controlled by the initial colloidal silica concentration. This particular method of catalyst preparation increased the Pt metal utilization, and generated a large amount of accessible voidage in the interpenetrating particle network of carbon and silica to support the facile transport of reactants and products. It was found that the Pt catalyst modified with silica at silica:Pt = 1.7:1 atomic ratio was more active than a catalyst prepared when silica to Pt ratio increased to 3.3:1.

#### References

- [1] H.S. Liu, C.J. Song, L. Zhang, J.J. Zhang, H.J. Wang, D.P. Wilkinson, *J. Power Sources* 155 (2006) 95–110.
- [2] A.S. Arico, S. Srinivasan, V. Antonucci, *Fuel Cells* 1 (2001) 1–29.
- [3] M.S. Wilson, H. Fernando, K.E. Stikafus, S. Gottesfeld, *J. Electrochem. Soc.* 140 (1993) 2872–2877.
- [4] D. Zhao, B.Q. Xu, *Phys. Chem. Chem. Phys.* 8 (2006) 5106–5114.
- [5] D. Zhao, B.Q. Xu, *Angew. Chem. Int. Ed.* 45 (2006) 4955–4959.
- [6] J.Y. Xi, J.S. Wang, L.H. Yu, X.P. Qiu, L.Q. Chen, *Chem. Commun.* (2007) 1656–1658.
- [7] J.H. Zeng, J.Y. Lee, J.J. Chen, P.K. Shen, S.Q. Song, *Fuel Cells* 7 (2007) 285–290.
- [8] B. Gurau, R. Viswanathan, R.X. Liu, T.J. Lafrenz, K.L. Ley, E.S. Smotkin, E. Redington, A. Sapienza, B.C. Chan, T.E. Mallonk, S. Sarangapani, *J. Phys. Chem. B* 102 (1998) 9997–10003.
- [9] R. Parsons, T. VanderNoot, *J. Electroanal. Chem.* 257 (1988) 9–45.
- [10] S.A. Lee, K.W. Park, J.H. Choi, B.K. Kwon, Y.E. Sung, *J. Electrochem. Soc.* 149 (2002) A1299–A1304.
- [11] X. Zhang, K.Y. Chan, *J. Mater. Chem.* 12 (2002) 1203–1206.
- [12] T.C. Deivaraj, W.X. Chen, J.Y. Lee, *J. Mater. Chem.* 13 (2003) 2555–2560.
- [13] A.S. Arico, A.K. Shukla, H. Kim, S. Park, M. Min, V. Antonucci, *Appl. Surf. Sci.* 172 (2001) 33–40.
- [14] M.-K. Min, J. Cho, K. Cho, H. Kim, *Electrochim. Acta* 45 (2000) 4211–4217.
- [15] N.S. Sobal, U. Ebels, H. Mohwald, M. Giersig, *J. Phys. Chem. B* 107 (2003) 7351–7354.
- [16] Y.M. Zhu, C.R. Cabrera, *Electrochem. Solid-State Lett.* 4 (2001) A45–A48.
- [17] J. Jiang, A. Kucernak, *J. Electroanal. Chem.* 533 (2002) 153–165.
- [18] Z.L. Liu, J.Y. Lee, M. Han, W.X. Chen, L.M. Gan, *J. Mater. Chem.* 12 (2002) 2453–2458.
- [19] J.H. Zeng, J.Y. Lee, *J. Power Sources* 140 (2005) 268–273.
- [20] J.H. Zeng, J.Y. Lee, *Int. J. Hydrogen Energy* 32 (2007) 4389–4396.